Nuclear Physics B100 (1975) 125–156

ON EXTRACTING THE DEEP INELASTIC STRUCTURE OF REGGEONS FROM HIGH-ENERGY MUON-PROTON EXPERIMENTS

N.S. CRAIGIE and G. SCHIERHOLZ
CERN, Geneva

Received 11 June 1975

We discuss how one can extract the reggeon structure functions from the inclusive distributions $\mu p \to \mu + H + X$, where H = p, n, $\Delta(N\pi)$, ... We concentrate mainly on the pion structure functions, which can be extracted from $\mu p \to \mu + n + X$ and $\mu p \to \mu + \Delta(N\pi) + X$, by virtue of the dominance of one-pion exchange (OPE). Here we include an estimate of the cross section and discuss in some detail the possible backgrounds, which, under certain plausible assumptions, we argue are small in an accessible experimental region, where the OPE cross section is largest. The discussion includes experimental tests for these backgrounds and procedures for disentangling the OPE from them, should they be important. We conclude by giving a possible experimental test of the validity of basic assumptions involved in showing that absorption corrections to OPE are small in the deep inelastic region.

1. Introduction

The advent of new very energetic muon beams with high luminosity at NAL and, in the near future, in the CERN Super Proton Synchroton (SPS) program, has opened the way to new kinds of measurements. In particular, it will be feasible to measure the inclusive distribution $\mu p \to \mu + H +$ anything, where the hadron H = p, n, Δ, K, ... is recoiling "slowly" in the lab system. In the appropriate kinematical region, these distributions give us valuable information on the deep inelastic structure of virtual hadron targets. In particular, it is possible to extract the pion structure functions in the space-like region, following the suggestion of Sullivan some time ago [1] The purpose of the present article, which is primarily addressed to experimentalists, is to discuss in some detail the kinematics and procedures involved in analysing these kinds of distributions. In particular, we shall discuss the problems involved in extracting the pion structure functions from the inclusive distributions $\mu p \to \mu + (\Delta, n) + X$, which make use of one-pion-exchange (OPE) dominance in a certain kinematical region. We shall discuss the Regge and absorption background in the case of the latter, pointing out that there exist accessible kinematical regions in which the OPE cross section is large and these backgrounds are relatively unimportant. We shall also mention some experimental tests for the background, and how one can

disentangle the OPE from, for example, the Regge exchange backgrounds in regions where the latter cannot be neglected. In the case of the absorption background, we shall show that, unlike other situations, in which one encounters OPE dominance, the absorption background is negligible in the deep inelastic region. This is based on the assumption that the electromagnetic structure of the pomeron is similar to other Regge exchanges, where we expect a form factor behaviour for the electroproduction of fixed-mass exclusive states (i.e. a particle or resonance). The absence of a form factor for the pomeron would imple, through the Drell-Yan relation [2], that the pomeron structure function will be singular as $\omega \to 1$.

As an introduction, we mention the theoretical interest in knowing the pion and reggeon structure functions. It is clear that the above kind of measurement will not be of high precision and, for example, we can probably hope to know at least the pion structure functions to about the 20–30% level. However, this accuracy is sufficient to give us valuable information on a number of outstanding theoretical questions concerning the deep inelastic structure of mesons. We give the following three examples:

(i) *Scaling in the space-like region.* This has become an interesting question, in view of the gross violation of scaling in the time-like region [3], in particular in the inclusive distribution $e^+e^- \to \gamma_v \to \pi + X$, which can be thought of as the crossed process to $\gamma_v \pi \to X$.

(ii) *Validity of the quark parton model.* This model [4] was constructed in order to describe the proton and neutron deep inelastic data, where it has been quite successful. However, so far the model has failed to describe to the same degree other processes involving currents [5]. It would therefore be desirable to examine the most closely related process, namely deep inelastic scattering off meson targets. The quark model alone makes a number of predictions (essentially from the SU(3) assignment), which can be expressed in the form of sum rules; for example (note that the pomeron cancels out):

$$\int_1^\infty \frac{d\omega}{\omega} \left[\tfrac{2}{3} F_2^p(\omega, q^2) - F_2^\pi(\omega, q^2)\right] = \frac{1}{9}, \qquad \omega = -\frac{2\nu}{q^2}. \tag{1.1}$$

In quark consistuent models [6,7] one can predict the threshold behaviour as $\omega \to 1$ and, for example,

$$\frac{F_2^p(\omega, q^2)}{F_2^\pi(\omega, q^2)} \underset{\omega \to 1}{\simeq} (\omega - 1)^P, \tag{1.2}$$

where in the dimensional counting analysis [6], $P = 2$, while (if one assumes $F_\pi(q^2) \to 1/|q^2|^{3/2}$ as $|q^2| \to \infty$) in the massive quark model [7], $P = 1$.

(iii) *Generalized crossing relations.* A number of attempts [8] have been made to connect the deep inelastic distribution $\gamma_v \pi \to X$ ($q^2 < 0$) to the e^+e^- annihilation inclusive distribution $\gamma_v \to \pi + X$ ($q^2 > 0$). Here one has to make some detailed assumptions about the underlying dynamics, which amount to simplifications and

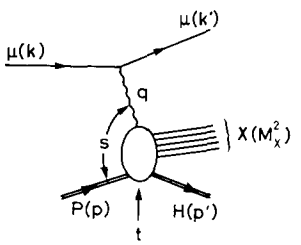

Fig. 1. Diagram giving the kinematics of $\mu p \to \mu + H + X$.

are supposed to be good approximations for large q^2. One such relation is the so-called reciprocity relation [9], which states that

$$\bar{F}_2(\omega, q^2) = \frac{1}{\omega^3} F_2(1/\omega, -q^2) , \tag{1.3}$$

where F_2 is the deep inelastic pion structure function and $\bar{F}_2$ is the corresponding structure function for the e^+e^- annihilation inclusive distribution. If (1.3) is used to predict the pion structure functions in the space-like region ($q^2 < 0$), using the SPEAR e^+e^- annihilation data [3] as input, then it would predict a drastic violation of scaling for large ω ($\omega > 2$) and, in fact, the pion structure function would be very large, for example $F_2^{\pi}(\omega, Q^2) > 25\, F_2^{p}(\omega, Q^2)$ for $\omega > 5$ and $Q^2 \simeq 20$.

Clearly, any information on (i) to (iii) above will be of great value in helping our theoretical understanding of the electromagnetic structure of hadrons.

We have divided the work up into five sections. In sect. 2 we discuss the kinematics and relevant dynamical functions, which are measured in the inclusive distribution $\mu p \to \mu + H + X$, where H is an arbitrary one-hadron state. In a particular kinematical domain we recall, in sect. 3, how these distributions are related to the reggeon structure functions through the Mueller-Regge model. In sect. 4 we discuss in some detail the problems of extracting the pion structure functions from the inclusive distributions $\mu p \to \mu + n + X$ and $\mu p \to \mu + \Delta^{++}(p\pi^+) + X$, in the region where OPE dominates. The discussion includes an estimate of the cross section and the level of the most important backgrounds. Finally, we mention in this section how one can experimentally test for these backgrounds and disentangle the OPE from them. Sect. 5 is devoted to the problem of the absorption background, where we give arguments as to why one can expect them to be small for large Q^2, except as $\omega \to 1$ (the resonance region). Finally, in sect. 6 we make some concluding remarks. In particular, we mention consequences for the inclusive distribution $\mu p \to \mu + p + X$, if the basic assumption we make in sect. 5 is not valid. Thereby, by measuring this distribution, we can test the validity of the latter.

2. Kinematics

In the one-photon exchange approximation the process

$$\mu(k) + \mathrm{p}(p) \to \mu(k') + \mathrm{H}(p') + \mathrm{X}$$

corresponds to fig. 1 and is described in terms of the following variables:

$$s = (p+q)^2 , \qquad Q^2 = -q^2 , \qquad M_{\mathrm{X}}^2 = (p+q-p')^2 , \qquad t = (p-p')^2 , \tag{2.1}$$

where $q = k - k'$.

It is also useful to define the scaling variables

$$\omega = \frac{2\nu}{Q^2} , \qquad \nu = p\cdot q , \qquad \omega' = \frac{2\nu'}{Q^2} , \qquad \nu' = (p-p')\cdot q . \tag{2.2}$$

In the lab system, where we define

$$p = (M_{\mathrm{p}}, \mathbf{0}) , \qquad q = (q_0, 0, 0, q) , \qquad p'_{\mathrm{L}} = (E'_{\mathrm{L}}, \boldsymbol{p}'_{\mathrm{L}}) ,$$

with

$$\boldsymbol{p}_{\mathrm{L}} = (p'_{\mathrm{L}} \sin\theta_{\mathrm{L}} \cos\varphi_{\mathrm{L}}, p'_{\mathrm{L}} \sin\theta_{\mathrm{L}} \sin\varphi_{\mathrm{L}}, p'_{\mathrm{L}} \cos\theta_{\mathrm{L}}) ,$$

we have

$$\nu = M_{\mathrm{p}} q_0 = M_{\mathrm{p}} [E_k - E_{k'}] ,$$

$$E'_{\mathrm{L}} \approx M_{\mathrm{H}} + p'^2_{\mathrm{L}}/2M_{\mathrm{H}} \qquad \text{for} \qquad |t| \ll M_{\mathrm{H}}^2 ,$$

where M_{H} is the mass of the detected hadron H,

$$p'^2_{\mathrm{L}} = \frac{M_{\mathrm{H}}}{M_{\mathrm{p}}} [(M_{\mathrm{H}} - M_{\mathrm{p}})^2 - t] ,$$

$$\omega' \approx \omega \left[1 - \frac{E'_{\mathrm{L}} - p'_{\mathrm{L}} \cos\theta_{\mathrm{L}}}{M_{\mathrm{p}}} \right] \qquad \text{for} \qquad \omega \gg 1 . \tag{2.3}$$

For large Q^2 the $t_{\min}$ of the inclusive distribution is given by

$$t_{\min} \approx -\left[\frac{\omega'^2 M_{\mathrm{p}}^2}{\omega(\omega - \omega')} + (M_{\mathrm{H}}^2 - M_{\mathrm{p}}^2) \frac{\omega'}{\omega - \omega'} \right] . \tag{2.4}$$

For $\omega \gg \omega'$ and H = p, n (equal-mass configurations),

$$t_{\min} \approx -\left(\frac{\omega'}{\omega} \right)^2 M_{\mathrm{p}}^2$$

for $\omega \gg \omega'$ and H = Δ

$$t_{\min} \approx -\frac{\omega'}{\omega} [M_{\Delta}^2 - M_{\mathrm{p}}^2] . \tag{2.5}$$

The main "tuning" variables for singling out kinematical regions in which a particular dynamical mechanism dominates, are

$$Q^2, t, M_X^2 \text{ or equivalently } t, \omega', \omega \,. \tag{2.6}$$

In general we will also be interested in H being a resonance, decaying into two or more hadrons; however, for the moment we shall take it to be a single-hadron state and discuss the generalizations involved, when we come to consider the case of a recoiling Δ. The cross section for detecting the outgoing muon and the recoiling hadron H is given in the lab system by

$$2E_{k'}E_{p'}\frac{d^6\sigma}{d^3k'd^3p'} = \frac{2\alpha^2}{Q^4(2\pi)^4 M_p E_k}\sum_{\text{spins}}|T|^2 \,,$$

where

$$\sum_{\text{spins}}|T|^2 = \tfrac{1}{2}\sum_{\substack{\text{muon}\\ \text{helicities}}}[\bar{u}(k')\gamma_\mu u(k)]\,[\bar{u}(k')\gamma_\nu u(k)]^+ W^{\mu\nu}(q,p,p') \,,$$

$$W^{\mu\nu}(q,p,p') = \tfrac{1}{2}\sum_{\substack{p,\,\mathrm{H}\\ \text{helicities}}}\sum_{\mathrm{X}}\int\prod_{i=1}^{n}\frac{d^3p_i}{(2\pi)^3 2E_i}(2\pi)^4\delta^4(q+p-p'-p_1-\ldots-p_n)$$

$$\times\langle p|J^\mu(0)|\mathrm{H},\mathrm{X}\rangle\langle\mathrm{H},\mathrm{X}|J^\nu(0)|p\rangle \,, \tag{2.7}$$

$$W^{\mu\nu}(q,p,p') = \sum_{i=1}^{5}\Gamma_i^{\mu\nu}V_i(s,q^2,M_X^2,t) \,, \tag{2.8a}$$

where

$$\Gamma_1^{\mu\nu} = q^\mu q^\nu - q^2 g^{\mu\nu} \,,$$

$$\Gamma_2^{\mu\nu} = (p^\mu q^\nu + p^\nu q^\mu)p\cdot q - p^\mu p^\nu q^2 - g^{\mu\nu}(p\cdot q)^2 \,,$$

$$\Gamma_3^{\mu\nu} = (p'^\mu q^\nu + p'^\nu q^\mu)p'\cdot q - p'^\mu p'^\nu q^2 - g^{\mu\nu}(p'\cdot q)^2 \,,$$

$$\Gamma_4^{\mu\nu} = (p'^\mu p^\nu + p'^\nu p^\mu)q\cdot p'q\cdot p - p'^\mu p'^\nu(p\cdot q)^2 - p^\mu p^\nu(p'\cdot q)^2 \,,$$

$$\Gamma_5^{\mu\nu} = i\left\{\left[p^\mu - \frac{p\cdot q}{q^2}q^\mu\right]\left[p'^\nu - \frac{p'\cdot q}{q^2}q^\nu\right] - \left[p'^\mu - \frac{p'\cdot q}{q^2}q^\mu\right]\left[p^\nu - \frac{p\cdot q}{q^2}q^\nu\right]\right\} \,.$$

We shall find it useful in the present case to introduce instead of V_2 corresponding to the covariant $\Gamma_2^{\mu\nu}$, a structure function V_2', which corresponds to the covariant tensor

$$\Gamma_2'^{\mu\nu} = (k^\mu q^\nu + k^\nu q^\mu)(k\cdot q) - k^\mu k^\nu q^2 - g^{\mu\nu}(k\cdot q)^2 \,, \tag{2.8b}$$

where $k = (p - p')$.

In the equivalent photon approximation we write (2.7) in the form [10]:

Table 1
Relationship between $H_{\lambda\lambda'}$ and V_i ($i = 1, ..., 4$) where $a^{(\pm)} = E'_L|q| \pm p'_L q_0$ and $\nu'_p = p' \cdot q$

$H_{\lambda\lambda'}$ \ V_i	1	2	3	4
++	q^2	ν^2	$\nu'^2_p - \frac{1}{2}q^2 p'^2_L \sin^2\theta_L$	$-\frac{1}{2}\nu^2 p'^2_L \sin^2\theta_L$
+−	−	−	$\frac{1}{2}q^2 p'^2_L \sin^2\theta_L$	$\frac{1}{2}\nu^2 p'^2_L \sin^2\theta_L$
+0	−	−	$-\sqrt{-\frac{1}{2}q^2}\, p'_L a^{(-)} \sin\theta_L$	$\sqrt{-\frac{1}{2}q^2}\, p'_L \nu a^{(+)} \sin\theta_L$
00	$-q^2$	$-M_p^2 q^2$	$-q^2 - p'^2_L \sin^2\theta_L + M_H^2$	$-q^2 a^{(+)2}$

$$2E_{p'}\frac{d^5\sigma}{d^3p'\,dQ^2\,ds} = 2\pi\Gamma_\epsilon 2E_{p'}\frac{d^3\sigma}{d^3p'}\,, \tag{2.9}$$

where

$$\Gamma_\epsilon = \frac{\alpha(s - M_p^2)}{16\pi^2 M_p^2 E_k^2 Q^2(1-\epsilon)}\,,$$

$$\epsilon = \left[1 + \frac{2q^2}{Q^2}\tan^2\tfrac{1}{2}\theta_\mu\right]^{-1}\,,$$

and $q^2 = \nu^2/M_p^2 + Q^2$, $\nu = M_p(E_k - E_{k'})$, $Q^2 = 4E_kE_{k'}\sin^2\frac{1}{2}\theta_\mu$; θ_μ is the angle between the incoming and outgoing muon in the lab system; $2E_{p'}(d^3\sigma/d^3p')$ describes the hadron H distribution resulting from the absorption by the proton of a virtual photon with fractional longitudinal polarization ϵ. We denote this distribution by $\gamma_v p \to H + X$. The latter cross section can be decomposed into the usual form, involving the cross section for absorption of transverse and longitudinal photons plus interference terms. In lab kinematics (2.3) this decomposition takes the form

$$2E_{p'}\frac{d^3\sigma}{d^3p'} = \frac{1}{\pi}\frac{E_{p'}}{p'}\left[\frac{d^2\sigma_U}{p'dp'\,d\cos\theta_L} + \epsilon\frac{d^2\sigma_L}{p'dp'\,d\cos\theta_L}\right.$$
$$\left. + \epsilon\frac{d^2\sigma_T}{p'dp'\,d\cos\theta_L}\cos 2\varphi_L + \sqrt{2\epsilon(\epsilon+1)}\frac{d^2\sigma_I}{p'dp'\,d\cos\theta_L}\cos\varphi_L\right]\,, \tag{2.10}$$

where

$$\frac{E_{p'}}{p'}\frac{d^2\sigma}{p'dp'\,d\cos\theta_L}^{U,L,T,I} = \frac{\alpha}{2\pi}\frac{1}{s - M_p^2}\,H_{++}, H_{00}, -H_{+-}, -2\,\mathrm{Re}\,H_{+0}\,,$$

$$H_{\lambda\lambda'} = \epsilon_\lambda^\mu \epsilon_{\lambda'}^{\nu *} W^{\mu\nu}(q, p, p')\,.$$

$H_{\lambda\lambda'}$ are the helicity structure functions in the lab system and reflect the dynamics.

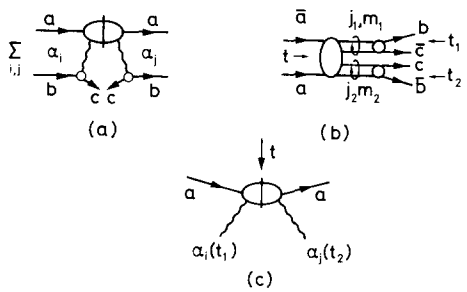

Fig. 2. (a) Mueller-Regge expansion of ab → c + X in the region $s/M_X^2 \gg$ and small t. (b) Corresponding cross-channel configuration, in which we have indicated the partial-wave expansions over (j_1, m_1) and (j_2, m_2) in the t_1 and t_2 channels. (c) The reggeon-particle four-point function $\alpha_i(t_1) + a \to \alpha_j(t_2) + a$.

[ϵ_λ^μ are the polarization vectors of the photon in a given polarization state $\lambda = (\pm, 0)$.] The relationship between the helicity structure functions $H_{\lambda\lambda'}$ and the covariant structure functions V_i $(i = 1, ..., 4)$ is given in table 1. If we integrate over the ϕ-distribution in eq. (2.10), the cross section can be written in the form

$$\frac{d^4\sigma}{dM_X^2 dt dQ^2 ds} = 2\pi\Gamma_\epsilon \left\{ \frac{d^2\sigma_U}{dM_X^2 dt} + \epsilon \frac{d^2\sigma_L}{dM_X^2 dt} \right\}$$

with

$$\frac{d^2\sigma_{U,L}}{dM_X^2 dt} = [4M_p\sqrt{(E_k - E_{k'})^2 + Q^2}]^{-1} \frac{\alpha}{2\pi(s - M_p^2)} \{H_{++}, H_{00}\} . \qquad (2.11)$$

3. The reggeon structure functions

It is now fairly well established that Regge theory extends to inclusive distributions in the appropriate limits. It is this fact, together with factorization of Regge poles, that allows us to single out, for example, in the present case, the reggeon deep inelastic structure functions, i.e. the structure functions associated with virtual hadron targets. Inclusive distributions are functions of a number of variables and have a number of different experimentally accessible asymptotic kinematical regions, in which different kinds of Regge behaviour emerge. These regions are singled out by using the variables, in the present case q^2, M_X^2 and t, as "tuning parameters".

We briefly recall the rudiments of Mueller-Regge theory [11]. The cross section for the inclusive distribution ab → c + X is determined by the appropriate missing-mass discontinuity of the six-point function abc → abc,

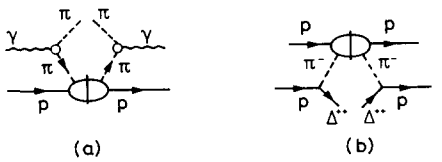

Fig. 3. (a) Mueller-Regge diagram for $\gamma p \to \pi + X$. (b) Mueller-Regge diagram for $pp \to \Delta^{++} + X$.

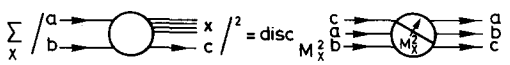

(3.1)

In the limit s/M_X^2 large and $t = (p_b - p_c)^2$ fixed at some small value, (3.1) reduces to a sum of Regge-pole exchange contributions (fig. 2a) plus possible non-factorizable background terms. This Regge-pole expansion corresponds to a particular crossed or t-channel configuration of the six-point function abc → abc, there being a number of different Regge-dominated s-channel domains (e.g., fragmentation and pionization regions), each corresponding to a different crossed channel. This is unlike the four-point function, for which there is a unique t-channel. The derivation of the Mueller-Regge expansion, starting from the partial-wave expansion in the appropriate crossed channel, has been treated in a number of works [12,13]. In particular, the double Regge limit is discussed in ref. [13], in which the helicity dependence of the external hadrons is considered. Here one starts with the partial-wave expansion in the t-channel configuration shown in fig. 2b, and after dealing with the problem of kinematic singularities, one makes a Gribov-Froissart projection of the partial-wave amplitudes, which allows one to carry out a Sommerfeld-Watson transform of the partial-wave summation. Consequently, in crossing to the s-channel, one finds in the region $(s/M_X^2) \to \infty$, t-fixed, that the inclusive distribution is dominated by the same Regge exchanges found in a corresponding analysis of the four-point function. The latter involves only Regge residues, i.e. vertex functions coupling the reggeons to the external hadrons. For an inclusive distribution, on the other hand, one has in addition the reggeon particle "scattering" amplitudes $A_{\alpha_i a \to \alpha_j a}(M_X^2, t, t_1, t_2)$, where t_1 and t_2 are the mass squared variables of the reggeons (fig. 2c). Present-day inclusive phenomenology provides useful information about the behaviour of such functions, the existence of which has already been implied by the presence of important Regge-cut corrections to exclusive processes [14] If we take only the leading term in the expansion shown in fig. 2a ($\alpha_i = \alpha_j = \alpha$), we obtain for the inclusive distribution ab → c + X (neglecting external helicity) a cross section of the form

$$2E_c \frac{d^3\sigma_{ab}}{d^3p_c} \underset{s/M_X^2 \gg 1}{=} \frac{1}{s} |\beta_{bc}^{\alpha}(t)|^2 \left(\frac{s}{M_X^2}\right)^{2\alpha(t)} M_X^2 \sigma_{\alpha a \to \alpha a}^{\text{tot}}(M_X^2) , \tag{3.2}$$

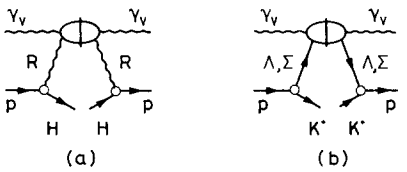

Fig. 4. (a) Mueller-Regge diagram for $\gamma_V p \to H + X$. (b) Mueller-Regge diagram for $\gamma_V p \to K^+ + X$.

where $\alpha^{\text{tot}}_{\alpha a \to \alpha a}(M_X^2)$ is the effective total cross section for αa elastic scattering (for small t one can usually neglect its t-dependence). Measuring the inclusive distribution $ab \to c + X$ for large s/M_X^2 allows one to extract this quantity, since the Regge residues β^{α}_{bc} are known from the corresponding exclusive process. For example, if we use the data on the pion-exchange-dominated inclusive processes (a) $\gamma p \to \pi^{\pm} + X$ [15] (see fig. 3a) and (b) $pp \to \Delta^{++} + X$ [16] (see fig. 3b), we obtain for $\sigma^{\text{tot}}_{\pi N}(M_X^2)$ values close to the known experimental (on shell) πN total cross section. This is essentially demonstrated in the analysis of refs. [17]...[18], respectively, where, by using the experimentally known $\sigma^{\text{tot}}_{\pi N}$ as input, one effectively reproduces the normalization in (a) and (b).

In the case of $\gamma_V(q^2)p \to H + X$, with H = p, n, Δ, ..., and restricting ourselves to the region, typically $(s/M_X^2) \to 6$, $|t| < 0.5\ \text{GeV}^2$ and $s/Q^2 > 10$ (we shall discuss later the important kinematical regions at NAL and SPS energies in some detail), the mechanism in fig. 4a is singled out, where

(a) for $H = p$, $R = \mathbb{P}, \pi^0, \rho, \ldots$

(b) for $H = n$, $R = \pi^+, \rho^+, \ldots$

(c) for $H = \Delta^{++}$, $R = \pi^-, A_2^-, \ldots$

If H is a strange meson, then R corresponds to a strange baryon exchange, as shown in fig. 4b for example.

Let us consider (a), (b), and (c) in the very small t-region, where pion and pomeron exchange are expected to dominate.

For (a) $\gamma_V p \to p + X$ we have

$$\frac{d^2\sigma_p}{dM_X^2 dt} = \frac{d^2\sigma_p^{P\cdot}}{dM_X^2 dt} + \frac{d^2\sigma_p^{\pi^0}}{dM_X^2 dt}\ , \tag{3.3}$$

where

$$\frac{d^2\sigma_p^R}{dM_X^2 dt} = \frac{1}{s^2} C_p^R(t)\left(\frac{s}{M_X^2}\right)^{2\alpha_R(t)} W^R(q^2, \omega', t)\ . \tag{3.4}$$

Since $C_p^R(t)$ depends on the lower vertices in fig. 4 and the reggeon signature factors, it is in principle always a known function of t (i.e. it can be extracted from the corresponding exclusive process). We shall define these quantities, in the case of the

OPE contribution to (b) and (c) in sect. 4. For (b) $\gamma_v p \to n + X$ we have OPE dominance, i.e.

$$\frac{d^2\sigma_n}{dM_X^2 dt} = \frac{d^2\sigma_n^{\pi^+}}{dM_X^2 dt} . \tag{3.5}$$

Similarly for the Δ^{++} and Δ^{+0} distributions (c), where we have

$$\frac{d^2\sigma_{\Delta^{++}}}{dM_X^2 dt} = \frac{d^2\sigma_{\Delta^{++}}^{\pi^-}}{dM_X^2 dt} , \quad \frac{d^2\sigma_{\Delta^{+0}}}{dM_X^2 dt} = \frac{d^2\sigma_{\Delta^{+0}}^{\pi^0}}{dM_X^2 dt} . \tag{3.6}$$

However, in the case of the Δ, the region in which the OPE dominates is strongly restricted by the t_{min} of the process (see eq. (2.5)). We shall discuss, in sect. 4, how the Δ-decay distribution can be used to disentangle the π-A_2 contributions in a region in which they overlap significantly.

For (a)–(c), the lower vertices in fig. 4 are known, so that an analysis of these inclusive distributions provides information on the pomeron and pion structure functions. In particular, a combined analysis will allow one to obtain information on the pion structure functions for different charge configurations. The importance of knowing the latter is evident from the recent SPEAR data [3] on the e^+e^- annihilation inclusive distributions $e^+e^- \to \gamma_v \to \pi^{\pm,0} + X$, where, although the π^0 distribution has not yet been measured directly, it is clear that it must show substantial deviations from the charged pion distributions (see ref. [3]). In the following sections, we shall discuss in some detail the problems involved in analysing the distributions (b) and (c) and the question of the absorption background, which has considerably complicated the detailed description of exclusive processes [19].

4. The pion structure functions

In this section we discuss in some detail how one can extract the pion structure functions from the above inclusive distributions. This involves disentangling the OPE from the A_2 (or ρ) and absorption backgrounds. We shall mention the various ways this can be accomplished and give some cross section estimates. We begin by considering the pure OPE contribution to (a) $\gamma_v p \to n + X$ (the equal-mass configuration) and (b) $\gamma_v p \to \Delta + X$. For the latter we initially treat the Δ as an elementary particle. Further our considerations apply to the region $s = 300$–600 GeV^2 and $Q^2 = 0$ to 20 GeV^2. The OPE dominates only at very small t-values and these are constrained by the t_{min}, which depends on ω or ω' or alternatively on Q^2 and M_X^2 (see eq. (2.4)). For the equal-mass configuration (a) this turns out to be a rather weak constraint, typically, when $\omega \gtrsim 5\omega'$ (for example $s = 300$, $Q^2 = 10$ and $M_X^2 = 60$), $|t_{min}| \leqslant 2m_\pi^2$). For the Δ, case (b), this ω' region would correspond to $|t_{min}| \lesssim 5m_\pi^2 = 0.1$ GeV^2, for which the A_2 contribution, although still small, starts to become important. However, at SPS energies, there is sufficient room to obtain

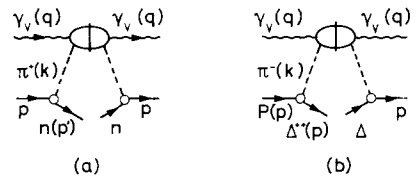

Fig. 5. (a) OPE contribution to $\gamma_V p \to n + X$. (b) OPE contribution to $\gamma_V p \to \Delta^{++} + X$.

$\omega > 10\omega'$, where the situation is correspondingly better. We shall discuss in detail these regions later.

4.1. Pure OPE contribution

For (a) $\gamma_V p \to n + X$, the full inclusive OPE-dominated structure function is given by (referring to fig. 5a):

$$W^{\mu\nu}(q,p,p') = \frac{1}{2} \sum_{\substack{p,n \\ \text{helicities}}} \left| q_{\pi pn} \frac{\bar{u}(p')\gamma_5 u(p)}{t - m_\pi^2} \right|^2 W_\pi^{\mu\nu}(q, p - p') , \tag{4.1}$$

where

$$W_\pi^{\mu\nu}(q,k) = \left[g^{\mu\nu} \frac{q^\mu q^\nu}{q^2} \right] W_1^\pi(\omega', q^2, k^2) + \left[k^\mu - \frac{k\cdot q}{q^2} q^\mu \right] \left[k^\nu - \frac{k\cdot q}{q^2} q^\nu \right]$$

$$\times \frac{1}{k^2} W_2^\pi(\omega', q^2, k^2) . \tag{4.2}$$

The apparent kinematic singularity at $t = k^2 = 0$ in the definition of (4.2) does not enter into the helicity structure functions $H_{\lambda\lambda'}$ defined in (2.10), which are given by

$$H_{++} = C_n^\pi(t)[W_1 + \tfrac{1}{2} W_2 \sin^2\theta] ,$$

$$H_{+-} = C_n^\pi(t)[-\tfrac{1}{2} W_2 \sin^2\theta] ,$$

$$\mathrm{Re}\, H_{+0} = C_n^\pi(t) \frac{\sin\theta}{\sqrt{2}} \frac{\omega'}{2} \sqrt{Q^2} \left[1 + \frac{\sqrt{-t}}{M_p} \right] W_2 ,$$

$$H_{00} = C_n^\pi(t)[W_1 - \tfrac{1}{2}\omega'\nu' W_2] ,$$

where

$$\nu' = k\cdot q = (p - p')\cdot q , \qquad t = k^2 ,$$

$$C_n^\pi(t) = g_{\pi pn}^2 \frac{(-t)}{(t - m_\pi^2)^2} . \tag{4.3}$$

Instead of (4.2), a more appropriate decomposition of $W_\pi^{\mu\nu}$ would be in terms of the causal structure functions V_1 and V_2' [20], defined in eqs. (2.8), which do not exhibit the apparent kinematic singularity at $t = k^2 = 0$. In the scaling region, we have

$$W_1(\omega', q^2, t) \xrightarrow[Q^2 \to \infty]{} F_1(\omega'),$$

$$\nu' W_2(\omega', q^2, t) \xrightarrow[Q^2 \to \infty]{} F_2(\omega'), \tag{4.4}$$

so that

$$H_{++} = C_n^\pi(t) F_1(\omega'),$$

$$H_{00} = C_n^\pi(t)[F_1(\omega') - \tfrac{1}{2}\omega' F_2(\omega')],$$

$$H_{+-} \sim O\left(\frac{1}{q^2}\right), \qquad \mathrm{Re}\, H_{+0} \sim O\left(\frac{1}{q^2}\right). \tag{4.5}$$

In (4.4) scaling implies that there is no t-dependence for finite t (i.e. $|t| \sim m_\pi^2$), so that $F_1(\omega)$ and $F_2(\omega)$ defined in (4.4) are in fact the physical pion structure functions in the scaling region. This, of course, assumes that there are no kinematic singularities (or zeros) in $W_1(\omega, q^2, t)$ and $W_2(\omega, q^2, t)$. However, if we had used, instead of (4.2) the decomposition in terms of the causal structure functions V_1 and V_2 [20], where no such singularities should emerge, we would arrive at the same results (4.4) and (4.5). The absence of the interference terms H_{+-} and $\mathrm{Re}\, H_{+0}$ for large q^2 means the ϕ distribution is flat. This can be used as a test of the OPE model or more generally of the dominance of pure Regge-pole exchange. For (b) $\gamma_V p \to \Delta^{++} + X$ (treating the Δ as an elementary spin-$\frac{3}{2}$ particle), (4.1) is replaced by (referring to fig. 5b):

$$W^{\mu\nu}(q, p, p') = \frac{1}{2} \sum_{\substack{p,\Delta \\ \text{helicities}}} \left| \frac{1}{m_\pi} G_{p\Delta\pi} U_\mu(p', \lambda_\Delta) k^\mu u(p, \lambda_p) \right|^2$$

$$\times \frac{1}{(t - m_\pi^2)^2} V_\pi^{\mu\nu}(q, p - p'), \tag{4.6}$$

where $U_\mu(p, \lambda)$ is the Rarita-Schwinger spinor and $k = p - p'$. Eq. (4.6) differs from (4.1) only by the structure of the lower vertex and we obtain for $H_{\lambda\lambda'}$ the same expressions as eqs. (4.3) and (4.5), with $C_n^\pi(t)$ replaced by

$$C_{\Delta^{++}}^{\pi^-}(t) = \tfrac{1}{3} G_{p\Delta\pi}^2 \frac{1}{m_\pi^2} [(M_\Delta + M_p)^2 - t] \frac{\lambda(M_\Delta^2, M_p^2, t)}{4M_\Delta^2} (t - m_\pi^2)^{-2}$$

$$\simeq \tfrac{4}{3}\pi \frac{G_{p\Delta\pi}^2}{4\pi} \frac{(M_\Delta + M_p)^2}{m_\pi^2} \frac{\lambda(M_\Delta^2, M_p^2, t)}{4M_\Delta^2} \frac{1}{(t - m_\pi^2)^2}. \tag{4.7}$$

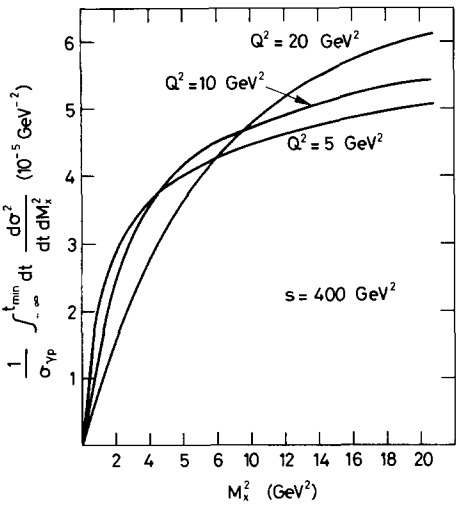

Fig. 6. Plot of $[\sigma^{tot}_{\gamma_v p}(Q^2, \omega)]^{-1} \int_{-\infty}^{t_{min}} dt d^2\sigma/(dM_X^2 dt)$ as a function of M_X^2, using the pion structure functions given in ref. [23].

For the distribution $\gamma_v p \to \Delta^{+0} + X$, we use

$$C^{\pi^0}_{\Delta^+ 0}(t) = \tfrac{2}{3} C^{\pi^-}_{\Delta^{++}}(t) . \tag{4.8}$$

We can estimate the cross section in a number of ways; however, perhaps the most useful estimate is as follows (concentrating on $\gamma_v p \to \Delta^{++} + X$):

$$\frac{d^2\sigma}{dM_X^2 dt} = \frac{1}{4M_p\sqrt{\nu^2/M_p^2 + Q^2}} \frac{1}{s - M_p^2} \frac{\alpha}{2\pi} [H_{++} + \epsilon H_{00}] , \tag{4.9}$$

with

$$H_{++} = C^{\pi^-}_{\Delta^{++}}(t) W_1^\pi(Q^2, \omega') ,$$

$$H_{00} = C^{\pi^-}_{\Delta^{++}}(t) [W_1^\pi(Q^2, \omega') - \tfrac{1}{2}\omega'\nu' W_2^\pi(Q^2, \omega')] .$$

Assuming the Callan-Gross relation [21], i.e. $H_{00} = 0$, we obtain for $0 < \omega'/\omega < 0.1$ $s \gg Q^2, M_X^2$:

$$\int dM_X^2 \int_{-\infty}^{t_{min}} \frac{d^2\sigma}{dM_X^2 dt} = \frac{4\pi^2\alpha}{Q^2} \left[\frac{1}{2\omega} \frac{1}{12\pi^2} \left(\frac{G^2_{p\Delta\pi}}{4\pi}\right)\left(\frac{M_\Delta + M_\rho}{m_\pi}\right)^2\right.$$
$$\left. \times \int_1^{10} d\omega' \nu' W_2^\pi(Q^2, \omega') \left[0.1 + \frac{\omega'}{\omega}\right]\right] . \tag{4.10}$$

Table 2
Values of $|t_{\min}|$, in units of m_π^2, for different Q^2 and M_X^2 (with $s = 300\ \mathrm{GeV}^2$)

M_X^2 \ Q^2	2	5	10
5	0.7	1	1.5
10	2	1.5	2
20	4	2.5	3

We can use eq. (4.10) to make the estimate, by inserting the value $G^2_{p\Delta\pi}/4\pi = 0.26$ and using a simple parametrization of $\nu W_2^\pi(Q^2, \omega) = F_2^\pi(\omega)$. This we assume [22] to rise linearly with ω from $\omega = 1$ to $\omega = 2$, and then to be a constant for $\omega > 2$. The constant is determined by $F_2^\pi(\omega) = \frac{2}{3}F_2^p(\omega)$ for large ω, which follows from Regge exchange in the large-ω region. For large ω, the total cross section for $\gamma_v p \to X$ is given by

$$\sigma^{\mathrm{tot}}_{\gamma_v p}(Q^2, \omega) \approx \frac{4\pi^2\alpha}{Q^2} F_2^p(\omega) \tag{4.11}$$

with $F_2^p(\omega) \to 0.35$ for $\omega \gg 1$ [23].

Putting this together and performing the integral in (4.10), we obtain the following rough estimate

$$\int_{Q^2}^{nQ^2} \mathrm{d}M_X^2 \int_{-\infty}^{t_{\min}} \mathrm{d}t \frac{\mathrm{d}^2\sigma_{\gamma_v p \to \Delta^{++}+X}}{\mathrm{d}M_X^2\,\mathrm{d}t} = \frac{1}{2\omega}\left[0.25 + \frac{12.5}{\omega}\right] \sigma^{\mathrm{tot}}_{\gamma_v p}(Q^2, \omega)\,. \tag{4.12}$$

For ω in the region 30–50, we see that the OPE contribution to $\gamma_v p \to \Delta^{++} + X$ accounts for (0.5–1.5%) of $\sigma^{\mathrm{tot}}_{\gamma_v p}$. If we add the contribution from $\gamma_v p \to \Delta^{+0} + X$, $\gamma_v p \to n + X$ and $\gamma_v p \to p + X$ (the latter including the pomeron exchange contribution), then these distributions account for approximately (5–10%) of $\sigma^{\mathrm{tot}}_{\gamma_v p}$ in the region $Q^2 = 5$–$20\ \mathrm{GeV}^2$ and $\nu = 100$–$300\ \mathrm{GeV}^2$. This means that about (5–10%) of the events in this region will be useful as far as measuring these distributions is concerned, assuming 100% detection efficiency.

For comparison, we have plotted in fig. 6 for $Q^2 = 5, 10, 20\ \mathrm{GeV}^2$, the quantity

$$C = \frac{1}{\sigma^{\mathrm{tot}}_{\gamma_v p}(Q^2, \omega)} \int_{-\infty}^{t_{\min}} \mathrm{d}t \frac{\mathrm{d}^2\sigma_{\gamma_v p \to \Delta^{++}+X}}{\mathrm{d}M_X^2\,\mathrm{d}t} \tag{4.13}$$

using as input the structure functions $\nu' W_2^\pi(Q^2, \omega')$ obtained in a model [24], which essentially predicts scaling. If, on the other hand, we use the reciprocity relation in ref. [9] (see eq. (1.3)), then the recent SPEAR data [3] would imply a substantial deviation from fig. 6 at large ω' and a drastically different variation with Q^2 for large M_X^2. Furthermore, the cross section would be much larger. One can

Table 3
Range of $|t - t_{min}|$ for which the value of $R < 20\%$ (see text)

s/M_X^2	$R < 20\%$ $\|t - t_{min}\|$ range	$R \sim 100\%$ $\|t\|$ (GeV^2)
10	$0-6\ m_\pi^2$	0.2
20	$0-4.5\ m_\pi^2$	0.3
60	$0-2.5\ m_\pi^2$	0.15

also expect deviations from fig. 6 for small Q^2 and M_X^2, due to resonance production in the $\gamma_v\pi$ system, which has yet to be studied.

4.2. The A_2 Regge background

The Δ-distribution is obtained by detecting the πN system, which causes quite a complication. However, the Δ-decay distribution provides a powerful tool for separating the OPE contribution from the A_2 exchange background. Before discussing this, we consider at what point one can expect the A_2 contribution to be important* We assume $W^\pi \simeq W^{A_2}$, so that A_2-exchange differs from OPE, in a simple Regge pole model, by the Regge factors and the lower vertex only, which are essentially known. From this it is simple to see that, for $\gamma_v p \to \Delta^{++} + X$, the ratio

$$R = 2E_{p'}\frac{d^3\sigma^{A_2}}{d^3p'} \Big/ 2E_{p'}\frac{d^3\sigma^{\pi}}{d^3p'} \tag{4.14}$$

is given by

$$R = \frac{\beta^2_{p\Delta A_2}(t)}{\beta^2_{p\Delta\pi}(t)}\,[\alpha'(t - m_\pi^2)]\left(\frac{s}{M_X^2}\right)^{2\alpha_{A_2}(0)} e^{\alpha t}\,, \tag{4.15}$$

where $\alpha_{A_2}(0) \simeq 0.4$ and $\alpha = 2(\alpha'_{A_2} - \alpha'_\pi)\log(s/M_X^2)$. From a naive quark model calculation, one expects $\beta_{p\Delta A_2} \simeq \beta_{p\Delta\pi}$. Now, since $|t_{min}| \simeq 0.6\ \omega'/\omega$, the t-region, in which R is small, is rather restricted and will require a rather accurate knowledge of t. We give in table 2 some typical values of $|t_{min}|$ for different Q^2 and M_X^2, taking $s = 300$ GeV^2. In table 3, we give the ranges of $|t - t_{min}|$ as a function of s/M_X^2 (with $s = 300$ GeV^2), for which $R < 20\%$, assuming $\alpha = 0$, this giving an upper limit, since there are indications that $\alpha'_{A_2} \gg \alpha'_\pi$ [26]. (In table 3 we also give the approximate value of $|t|$, for which $R \simeq 100\%$).

From table 3 we see that if one works close to $t - t_{min}$, with a bin size of approximately $\Delta t \sim m_\pi^2$, one can always single out OPE from the A_2 Regge background to about the 20% level. For comparison, we plot in fig. 7a and b the OPE and A_2

* The ρ-contribution is known to be small compared to the A_2 contribution, see e.q. ref. [25].

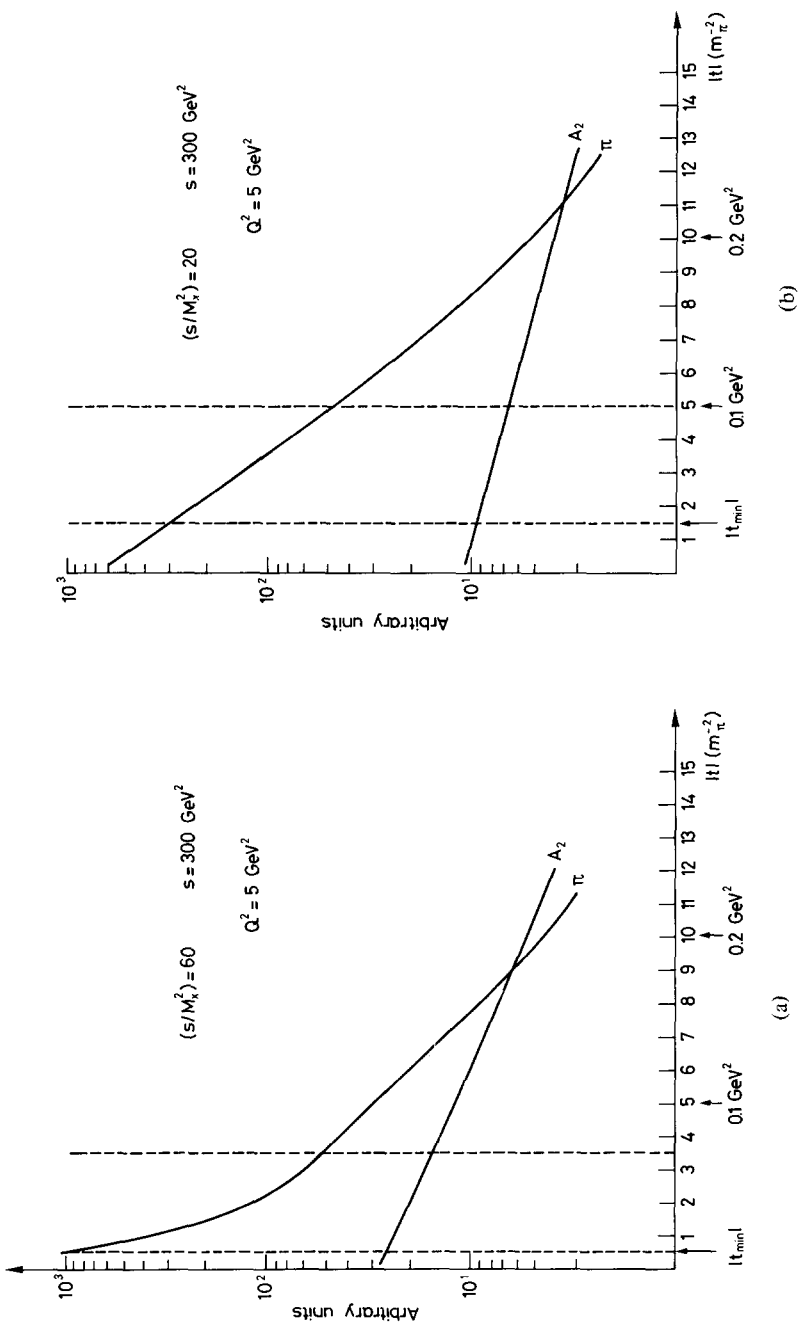

Fig. 7. (a) and (b) show a comparison of the π and A_2 contributions to $\gamma_V p \to \Delta + X$ for two values of M_X^2, namely $M_X^2 = 5$ and 15 GeV^2, respectively.

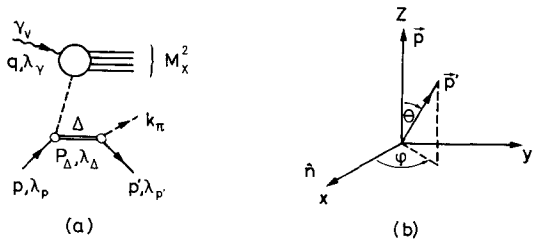

Fig. 8. (a) π (or A_2) exchange contribution to $\gamma_V p \to \Delta(N\pi) + X$. (b) Definition of Δ-decay angles in the Gottfried-Jackson system.

contributions for the extreme cases $s/M_X^2 = 20$ and $s/M_X^2 = 60$. These correspond to $M_X^2 \sim 15$ GeV^2 and $M_X^2 \sim 5$ GeV^2 respectively, choosing $s = 300$ GeV^2 and $Q^2 \simeq 5$ GeV^2.

4.3. The Δ-decay distribution

We now turn to the Δ-decay distribution; since the Δ has to be reconstructed from a πN final state, one in fact measures the double inclusive distribution $\gamma_V p \to \pi p + X$, where the πp system has invariant mass $M^{*2} \simeq M_\Delta^2$ and is recoiling "slowly" in the lab system.

For a particular missing-mass state X, fig. 8a corresponds to a production amplitude of the following form, using the resonance approximation:

$$T(\gamma_V p \to p\pi + X) = T(\gamma_V p \to \Delta + X) \frac{1}{M^{*2} - M_\Delta^2 + iM_\Delta \Gamma_\Delta} T(\Delta \to \pi p) , \quad (4.16)$$

where $M^{*2} = (p' + k_\pi)^2$.

Summing over the missing-mass states we obtain for the two-particle distribution $\gamma_V p \to p\pi + X$

$$2E_{p'} 2E_\pi \frac{d^6\sigma}{d^3p' d^3k_\pi} = [\text{flux factor}] \sum_{\lambda\gamma\lambda p} \sum_X |T(\gamma_V p \to \Delta + X)|^2$$

$$\times \frac{1}{(M^{*2} - M_\Delta^2)^2 + M_\Delta^2 \Gamma_\Delta^2} \sum_{\lambda_{p'}} |T(\Delta \to \pi p)|^2 . \quad (4.17)$$

Since the Δ can be produced in different helicity states, for a given initial proton helicity, depending on the production mechanism, we make use of the density matrix formalism in the Gottfried-Jackson system [27]. In the latter system the helicities are defined in the rest frame of the Δ, with the spin quantized along the initial proton direction (chosen to be the z-axis) as shown in fig. 8b. In terms of the density matrices, we write

$$\sum_{\lambda_\gamma \lambda_p} \sum_{\mathrm{X}} T_{\lambda_\Delta}(\gamma_\mathrm{v} \mathrm{p} \to \Delta + \mathrm{X}) T^*_{\lambda'_\Delta}(\gamma_\mathrm{v} \mathrm{p} \to \Delta + \mathrm{X}) = \rho_{\lambda_\Delta \lambda'_\Delta} \sum_{\lambda_\gamma \lambda_p \lambda_\Delta} \sum_{\mathrm{X}} |T_{\lambda_\Delta}|^2 , \tag{4.18}$$

where λ_Δ and λ'_Δ refer to the Δ-helicities of the respective production amplitudes entering in the right-hand side of eq. (4.18). The decay distribution of the Δ in the helicity frame (i.e. the Gottfried-Jackson system), is given by

$$R_{\lambda_\Delta \lambda'_\Delta}(\theta, \varphi) = \frac{4}{4\pi} \sum_{\lambda_{p'} = \pm 1/2} |T^{3/2}_{\lambda_p}(\Delta \to \mathrm{p}\pi)|^2 D^{3/2}_{\lambda_\Delta \lambda_{p'}}(\theta, \varphi) D^{3/2}_{\lambda'_\Delta \lambda_{p'}}(\theta, \varphi) . \tag{4.19}$$

Since $|T^{3/2}_{\lambda_p}|^2 = |T^{3/2}_{-\lambda_p}|^2$ from parity conservation, we can rewrite eq. (4.19) in the form

$$R_{\lambda_\Delta \lambda'_\Delta}(\theta, \varphi) = A_{\lambda_\Delta \lambda'_\Delta}(\theta, \varphi) \sum_{\lambda_{p'}} |T(\Delta \to \pi \mathrm{p})|^2 ,$$

where

$$A_{\lambda_\Delta \lambda'_\Delta}(\theta, \varphi) = \sum_{\lambda_{p'} = \pm 1/2} D^{3/2}_{\lambda_\Delta \lambda_{p'}}(\theta, \varphi) D^{3/2}_{\lambda'_\Delta \lambda_{p'}}(\theta, \varphi) . \tag{4.20}$$

We now change the variables from

$$\frac{\mathrm{d}^3 p'}{2E_{p'}} \frac{\mathrm{d}^3 k_\pi}{2E_\pi} \quad \text{to} \quad \mathrm{d}M^2_\mathrm{X} \mathrm{d}t \mathrm{d}\Omega_\Delta k_\pi \mathrm{d}k_\pi \tag{4.21}$$

and integrate out the k_π dependence and obtain

$$\frac{\mathrm{d}\sigma}{\mathrm{d}M^2_\mathrm{X} \mathrm{d}t \mathrm{d}M^{*2} \mathrm{d}\Omega_\Delta} = \frac{\mathrm{d}^2 \sigma}{\mathrm{d}M^2_\mathrm{X} \mathrm{d}t} \frac{M_\Delta \Gamma_\Delta}{(M^{*2} - M^2_\Delta)^2 + M^2_\Delta \Gamma^2_\Delta} W(\theta, \varphi) , \tag{4.22}$$

where

$$W(\theta, \varphi) = \mathrm{Tr}\{\rho A(\theta, \varphi)\} ,$$

$$M_\Delta \Gamma_\Delta = \sum_{\lambda_{p'}} \int \frac{\mathrm{d}^3 p'}{(2\pi)^3 2E_{p'}} \frac{\mathrm{d}^3 k_\pi}{(2\pi)^3 2E_\pi} |T(\Delta \to \pi(\mathrm{p})|^2 \delta^4(p_\Delta - p' - k_\pi)(2\pi)^4 ,$$

and $\mathrm{d}^2\sigma/\mathrm{d}M^2_\mathrm{X}\mathrm{d}t$ is just the cross section for $\gamma_\mathrm{v} \mathrm{p} \to \Delta + \mathrm{X}$ in the approximation $P^2_\Delta = N^2_\Delta$. The general form of the angular distribution function $W(\theta, \phi)$ is given by [27]:

$$W(\theta, \varphi) = \frac{3}{4\pi} [\rho_{33} \sin^2\theta + \rho_{11}(\tfrac{1}{3} + \cos^2\theta) - 2\sqrt{\tfrac{1}{3}} \,\mathrm{Re}\, \rho_{3-1} \sin^2\theta \cos^2\varphi$$

$$- 2\sqrt{\tfrac{1}{3}} \,\mathrm{Re}\, \rho_{31} \sin^2\theta \cos\varphi] . \tag{4.23}$$

For the OPE mechanism, eq. (4.23) considerably simplifies, since, by choosing the t-channel helicity system, one readily sees that only one helicity configuration survives, so that, in converting back to the Gottfried-Jackson system, it is simple to see that

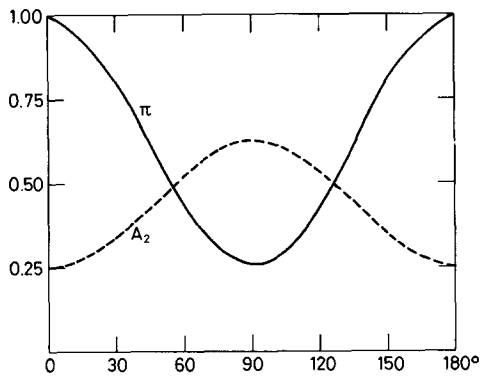

Fig. 9. The Δ-decay distribution (integrated over ϕ) for π (solid curve) and A_2 (dotted curve), respectively.

$$\rho_{11} = \tfrac{1}{2} \qquad \text{and} \qquad \rho_{33} = \rho_{31} = \rho_{3-1} = 0 \tag{4.24}$$

and hence

$$W^{\pi}(\theta, \varphi) = \frac{1}{8\pi} [1 + 3\cos^2\theta] . \tag{4.25}$$

For the A_2 exchange, the situation is more complicated, and one usually argues on the basis of ρ-A_2 exchange degeneracy, that its angular distribution will be the same as that for ρ-exchange. For the latter, which was first considered by Stodolsky and Sakurai [28], it turns out that the decay distribution is simplest when one quantizes the spin along the normal to the production plane. It is then argued that the $N\rho N^*$ vertex behaves like $N\gamma N^*$ (for example on the basis of vector dominance), so that we have a pure M_{1+} excitation, which means that the production of $\pm\frac{3}{2}$ helicity states along this axis is negligible. In terms of the decay angles (θ', ϕ'), defined with respect to the normal to the production plane, the angular distribution is simply given by

$$W^{\rho}(\theta', \varphi') = \frac{1}{8\pi} [1 + 3\cos^2\theta'] . \tag{4.26}$$

We can convert back to the helicity angles (θ, ϕ) by making a simple rotation through $\frac{1}{2}\pi$ about the y-axis and using the following transformation properties of the density matrices under rotation:

$$\rho_{\lambda\lambda'} = \sum_{nn'} \rho'_{nn'} D^{3/2}_{\lambda n}(\alpha, \beta, \gamma) D^{3/2\,*}_{\lambda' n'}(\alpha, \beta, \gamma) . \tag{4.27}$$

The Stodolsky-Sakurai distribution corresponds in the (θ, ϕ) system to

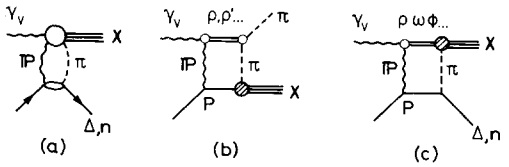

Fig. 10. (a) Absorption corrections to $\gamma_V p \to \Delta, n + X$. (b) Absorption corrections to $\gamma p \to \pi + X$. (c) Resonance contribution to diagram (a).

$$\rho'_{nn'} = \delta_{\frac{1}{2}n}\delta_{\frac{1}{2}n'} + \delta_{-\frac{1}{2}n}\delta_{-\frac{1}{2}n'} ,$$

so that using eq. (4.27) with $\alpha = \gamma = 0$, and $\beta = \frac{1}{2}\pi$, one sees that

$$\rho_{33} = \tfrac{3}{8} , \quad \rho_{11} = \tfrac{1}{8} , \quad \rho_{3-1} = \tfrac{1}{8}\sqrt{3} , \quad \rho_{31} = 0 , \tag{4.28}$$

and correspondingly

$$W^p(\theta, \varphi) = \frac{1}{16\pi}[5 - 3\cos^2\theta - 3\sin^2\theta\cos^2\varphi] . \tag{4.29}$$

For the reasons mentioned above, the A_2-distribution is expected to be approximately the same. This is confirmed in a static Chew-Low type calculation for N* production via A_2 exchange by Hara [29]. Furthermore, it seems to work empirically, for example in the reactions $Kp \to K^0\Delta^{++}$, which is ρ-A_2 dominated † and $\pi^- p \to \Delta^{++}\eta^0$, which is pure A_2 dominated [31]. The marked difference between the two decay distribution (4.25) and (4.28) (see fig. 9) allows one to disentangle the π and A_2 exchanges, even in a region in which they overlap, providing the statistics on the decay distribution is high enough. Here one would use the following decomposition of the full cross section, neglecting π-A_2 interference terms, which are likely to be small (see appendix):

$$\frac{d\sigma}{dM_X^2 dt dM^{*2} d\Omega(\theta, q)} = \frac{M_\Delta \Gamma_\Delta}{(M^{*2} - M_\Delta^2)^2 + M_\Delta^2 \Gamma_\Delta^2} \left[\frac{d^2\sigma^\pi}{dM_X^2 dt} W^\pi + \frac{d^2\sigma^{A_2}}{dM_X^2 dt} W^{A_2}\right] . \tag{4.30}$$

By choosing suitable missing-mass bins ΔM_X^2 and integrating over t, one can make a maximum likelihood fit to the angular distribution in (4.30) in order to obtain the coefficients $d^2\sigma^\pi/dM_X^2 dt$ and $d^2\sigma^{A_2}/dM_X^2 dt$. Experience shows that, for each missing-mass bin, about 500 to 1000 events would be adequate for such an analysis [32]

† For the ρ-A_2 exchange degeneracy, see ref. [30].

4.4. Absorption background

The second kind of background that one might expect to accompany the OPE mechanism for $\gamma_v p \to (\Delta, n) + X$, are absorption effects, which can generally be understood in terms of a P-π cut contribution of the form shown in fig. 10a. In the next section, we shall give arguments as to why we can expect this kind of mechanism to be suppressed in the deep inelastic limit and under certain plausible assumptions, in fact to decrease like $M_X^{-2} = 1/(\omega' - 1)Q^2$. However, there are two different experimental tests that can be made for this background, even in the presence of A_2 exchange. Before discussing these tests, we mention here briefly a reason why one can expect the physics of the absorption corrections to the OPE contribution to the deep inelastic processes $\gamma_v p \to \Delta, n + X$, to be quite different from that in other situation, in which one encounters OPE dominance. As an example, let us consider the photo-induced process $\gamma p \to \pi^{\pm} + X$ in the photon fragmentation region, where γ is a real photon. Here a good case can be made for attributing the absorption corrections to $\rho, \rho', \ldots$, diffractive intermediate states [33] (fig. 10b). However, if we insert diffractively excited intermediate states in fig. 10a, which corresponds to fig. 10c, then we expect the contributions from the lower-lying states ρ, ω and ϕ to die out with Q^2 because of their form factors. This means that only the higher-lying states or, more realistically, only a continuum with an invariant mass growing like Q^2 contributes. The quark parton model has been used to describe the latter situation; however, this involves highly fictitious quark-hadron scattering amplitudes, to which it is difficult to attach any physical intuition. It is therefore correspondingly difficult to discuss absorption corrections within the context of this model. On the other hand, the arguments we offer in the next section are somewhat less model-dependent, depending essentially on one assumption, which itself can be experimentally checked. We might mention also here that it is sometimes argued that absorption corrections to OPE are only important for the equal-mass configuration, in our case $\gamma_v p \to n + X$, since these are always proportional to $(-t)$ and thus vanish as $t \to 0$, which is not the case for $\gamma_v p \to \Delta + X$. If the Regge cut correction to the latter has the same order of magnitude as that in the equal-mass configuration (which might, for example, be parametrized by the so-called poor man's absorption model [30], in which $(-t)$ is replaced by $(m_\pi + \sqrt{-t})^2$), then it is simple to see that the cut will be negligible in the case of $\gamma_v p \to \Delta + X$. However, this amounts to little more than a guess, and we shall not pursue this possibility further, since the arguments we offer in the next section are independent of the lower vertex in fig. 10a and therefore apply equally to both cases.

In the case of $\gamma_v p \to \Delta + X$, one can carry out two independent tests for the presence of a non-Regge pole background, even when the A_2 exchange is non-negligible. For the equal-mass configuration $\gamma_v p \to n + X$, only the first test is relevant, since the second concerns the Δ-decay distribution.

4.4.1. The angular distribution in the laboratory system. We return to the general

decomposition (eq. (2.10)) of the cross section $2E_{p'}\mathrm{d}^3\sigma/\mathrm{d}^3p'$ for $\gamma_v p \to H + X$, in terms of the helicity structure functions $H_{\lambda\lambda'}$ in the lab system, in which the momentum of the detected hadron is defined by

$$p'_L = (p'_L \sin\theta_L \cos\varphi_L, p'_L \sin\theta_L \sin\varphi_L, p'_L \cos\theta_L) , \tag{4.31}$$

$$t \approx (M_H - M_p)^2 - \frac{M_p}{M_H} p'^2_L ,$$

where $M_H = M_\Delta$ or M_p, and

$$\omega' = \omega\left[1 - \frac{E'_L - p'_L \cos\theta_L}{M_p}\right] , \tag{4.32}$$

which are independent of the azimuthal angle ϕ_L. We saw that, in the deep inelastic region, the OPE mechanism leads to

$$H_{++} = c_\pi(t) W^\pi_A(\omega', Q^2) ,$$

$$H_{00} = c_\pi(t) F^\pi_L(\omega', Q^2) ,$$

where

$$F^\pi_L = W^\pi_1 - \tfrac{1}{2}\omega'\nu' W^\pi_2 ,$$

$$H_{+-} \propto \frac{1}{Q^2}[H_{++} + \epsilon H_{00}] , \qquad \mathrm{Re}\, H_{+0} \propto \frac{1}{Q^2}[H_{++} + \epsilon H_{00}] . \tag{4.33}$$

Hence the ϕ_L distribution will be flat. This property depends crucially on the factorization property of the Regge poles, which means pure Regge-pole exchange will only contribute to the structure functions V_1 and V'_2. However, the presence of a non-factorizable background would lead to contributions to V_3 and V_4 as well, and if these are significant for large Q^2, then by examining the relationship between the V_i ($i = 1, 4$) and the helicity structure functions (table 1), we see that in general

$$H_{+-} , \qquad \mathrm{Re}\, H_{+0} \propto [H_{++} + \epsilon H_{00}] , \tag{4.34}$$

as far as the Q^2 dependence is concerned. A measure of the non-factorizable or absorptive background is therefore given by

$$|H_{+-}|/[H_{++} + \epsilon H_{00}] \qquad \text{and} \qquad |\mathrm{Re}\, H_{+0}|/[H_{++} + \epsilon H_{00}] , \tag{4.35}$$

which can be extracted from the ϕ_L dependence.

4.4.2. The density matrices and the Treiman-Yang test. In the case of $\gamma_v p \to \Delta + X$, if we look at the Δ-decay distribution in the Gottfried-Jackson system, then the absence of any ϕ-dependence corresponds to pure OPE. This is the so-called Treiman-Yang test [34]. Pure OPE implies

$$\rho_{33} = \rho_{31} = \rho_{3-1} = 0 , \qquad \rho_{11} = \tfrac{1}{2} , \tag{4.36}$$

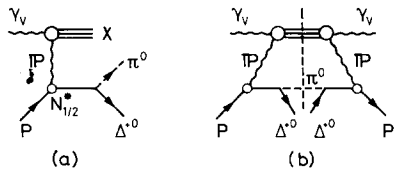

Fig. 11. An additional background to $\gamma_v p \to \Delta^{+0} + X$.

whereas the A_2 contribution corresponds to

$$\rho_{33} = \tfrac{3}{8}\,, \qquad \rho_{3-1} = \tfrac{1}{8}\sqrt{3}\,, \qquad \rho_{31} = 0\,, \qquad \rho_{11} = \tfrac{1}{8}\,. \tag{4.37}$$

Hence, even if the A_2 contribution is present, a significant deviation from $\rho_{31} = 0$ would indicate the presence of an additional background. If such a background were present, then one could work close to $t = t_{\min}$, so that the A_2 contribution is below the 20% level, in order to see if there is a significant deviation from (4.36) by measuring the angular distribution. In this way, one can ascertain the importance of any absorption corrections to OPE.

Tests (a) and (b) are sufficient to check OPE dominance in the presence of both a Regge pole and Regge cut backgrounds. In summary, pure OPE corresponds to

(i) No dependence of $2E_L d^3\sigma/d^3p_L$ on ϕ_L;

(ii) No dependence on the azimuthal angle ϕ of the Δ-decay distribution in the Gottfried-Jackson system;

(iii) $W^{\pi}(\theta) = \frac{1}{8}[1 + 3\cos^2\theta]$, i.e. $\rho_{33} = \rho_{31} = \rho_{3-1} = 0$.

Although these tests should be made, statistics permitting, as we have suggested above, in a limited kinematical region in which the cross section is at its maximum, these backgrounds are likely to be small, i.e. at the 20% level or even less. Before we give arguments as to why we expect the Regge cut background to be small, we should perhaps mention one other source of background in the case of $\gamma_v p \to \Delta^{+0} + X$. If the diffractive excitation mechanism in fig. 11a is important and the π^0 is not detected, then this will appear to contribute to the latter distribution. This kind of mechanism involves the pomeron structure functions of fig. 11b and, at least for large M_X^2, we can expect it to be negligible, because the triple-pomeron coupling is relatively small. Nevertheless the above tests can be used to distinguish the OPE from this kind of background, because it falls under the non-factorizable category.

5. Estimate of the absorption corrections to the deep inelastic OPE mechanism

We consider here the various ways in which absorption corrections to the OPE contribution ot $\gamma_v p \to \Delta$, n + X are built up, for large Q^2. We have already hinted that the physics involved is somewhat different than in other situations, where one encounters OPE dominance, essentially because of the deep inelastic structure of

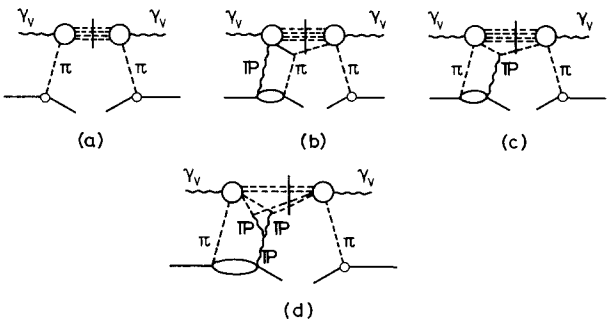

Fig. 12. (a) Pure-OPE term. (b) and (c) Initial- and final-state absorption corrections. (d) Diagram involving pomeron coupling to more than one particle in deep inelastic continuum.

the production mechanism. The general structure of the Regge-cut contributions we shall be considering is shown in fig. 12b and c. Fig. 12a depicts the pure OPE contribution.

We consider first the influence of these initial- and final-state absorption corrections on the pure OPE, based on the assumption that the pomeron couples to single-hadron states in the continuum. For example for the pomeron, we know this is a good approximation from high-energy nuclei collisions [35]. The main corrections come from diagrams like that of fig. 12d, which are relatively unimportant by virtue of the small size of the effective triple-pomeron coupling [36]. We begin by concentrating on pomeron exchange in the final state. Referring to fig. 12c, we write the pion structure function in the form

$$W_\pi^{\mu\nu} = \frac{1}{n_\pi}\int \frac{\mathrm{d}^3k'}{(2\pi)^3 2E_{k'}} W_{(3)}^{\mu\nu}(q, k, k', k - k'') , \tag{5.1}$$

where n_π is the multiplicity of the final state X and $W_{(3)}^{\mu\nu}$ is the missing-mass discontinuity of the six-point function, depicted in fig. 13a and defined by

$$W_{(3)}^{\mu\nu}(q, k, k', k - k'') = \sum_{\mathrm{X}} \langle \pi(k')|J_{(0)}^{\mu}|\pi(k''), \mathrm{X}\rangle\langle \pi(k''), \mathrm{X}|J_{(0)}^{\mu}|\pi(k)\rangle \tag{5.2}$$

$$= \sum_i \Gamma_i^{\mu\nu} \mathcal{V}^i(Q^2, s', s'', K_{\mathrm{X}}^2, \bar{t}, \bar{t}') , \tag{5.3}$$

where

$$s' = (q + k)^2 ,$$
$$s'' = (q + k'')^2 ,$$
$$K_{\mathrm{X}}^2 = (q + k - k')^2 ,$$
$$\bar{t} = (k - k')^2 = (k'' - k''')^2 , \qquad \bar{t}' = (k' - k''')^2 . \tag{5.4}$$

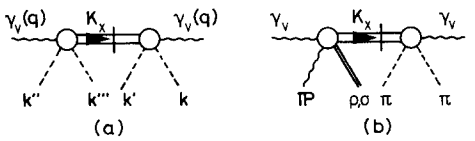

Fig. 13. (a) Non-forward missing-mass discontinuity of the six-point functions $\gamma_V(q) + \pi(k'') + \pi(k') \to \gamma_V(q) + \pi(k'') + \pi(k)$. (b) Missing-mass discontinuity of the six-point function $\gamma_V + P + \pi \to \gamma_V + R + \pi$, $R = \rho, \sigma, \ldots$.

The first four covariants are the same as those defined in eq. (2.8), with k and k' substituted for p and p', respectively. The remaining ones are constructed in the same way, using the vector $k - k''$ plus crossed terms involving this vector, k and k'. The latter vanish as $k'' \to k$. After performing the phase-space integral in (5.1), the whole expression reduces to the form

$$W_\pi^{\mu\nu}(q, k) = \Gamma_1^{\mu\nu} V_1^\pi + \Gamma_2^{\mu\nu}(q, k) V_2^\pi \,. \tag{5.5}$$

If we return to the whole process $\gamma_V p \to \Delta$, n + X, fig. 12a then factorizing at the pion pole, we see that the OPE contribution corresponds to

$$W_{\mathrm{OPE}}^{\mu\nu}(q, p, p') = \Gamma_1^{\mu\nu} V_1 + \Gamma_2^{\mu\nu}(q, p, p') V_2' \,,$$

where

$$V_i = |V_{\mathrm{pH}\pi}(t)|^2 |\Delta_\pi(t)|^2 V_i^\pi(Q^2, s') \,, \qquad i = 1, 2 \,, \tag{5.6}$$

and $V_{\mathrm{pH}\pi}(t)$ describes the lower vertex $[H = \Delta, \mathrm{n}]$ and $\Delta_\pi(t)$ is the pion propagator.

The corresponding expression for the absorption correction (fig. 12c) is given by

$$W_{\mathrm{abs}}^{\mu\nu}(q, p, p') = V_{\mathrm{pH}\pi}(t) \Delta_\pi(t) \int \frac{\mathrm{d}^4 k''}{(2\pi)^4} A_{\mathrm{pH}}^{\pi\mathbb{P}}(s_0, t, t_1, t_2)$$

$$\times \Delta_\pi(t_1)\, \mathbb{P}(t_2, s/s'') G_{\pi\pi\mathbb{P}} \int \frac{\mathrm{d}^3 k'}{(2\pi)^3 2E_{s'}} W_{(3)}^{\mu\nu}(q, k, k', k - k'') \Delta_\pi(k'''^2) \,, \tag{5.7}$$

where

$$s_0 = (p - k'')^2 \,, \qquad t_1 = k^2 \,, \qquad t_2 = (k - k'')^2 = (k' - k''')^2 \,,$$

and

$$\mathbb{P}(t_2, s/s'') = i(s/s'')^{\alpha_\pi(A_2)} \,.$$

The amplitude $A_{\mathrm{pH}}^{\pi\mathbb{P}}$ describes the four-point function $\pi p \to \mathrm{PH}$ and $G_{\pi\pi,\mathrm{P}}$ is the pion-pomeron vertex. For $s \gg s', s'', Q^2$ (i.e. the kinematical region, in which we are interested), we can make the change of variables

$$\mathrm{d}^4 k'' = \frac{1}{4s} \frac{\theta(\lambda(t, t_1, t_2))}{\lambda^{1/2}(t, t_1, t_2)} \mathrm{d}t_1 \mathrm{d}t_2 \mathrm{d}s'' \mathrm{d}s_0 \,. \tag{5.8}$$

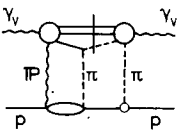

Fig. 14. Diagram which would lead to a violation of scaling in $\gamma_V p \to X$ if diagram 13b violates scaling.

The various covariants in (5.3) clearly contribute with similar weight in the integral (5.7) and lead to contributions to all the structure functions $\{V_i\}$ defined in (2.8). For simplicity, we concentrate on the term $\Gamma^{\mu\nu}(q,k)\mathcal{V}_2$, which contributes only to the structure function V_2'. Here we obtain

$$V'_{2\mathrm{abs}} = \frac{V_{\mathrm{pH}\pi}(t)\Delta_\pi(t)}{16s(2\pi)^6\lambda^{1/2}(s',q^2,m_\pi^2)}\int\frac{\mathrm{d}t_1\,\mathrm{d}t_2\theta(\lambda)}{\lambda^{1/2}(t,t_1,t_2)}N^{\pi\mathbb{P}}_{\mathrm{pH}}(t,t_1,t_2)$$

$$\times G_{\pi\pi\mathbb{P}}\Delta_\pi(t_1)\int\mathrm{d}s''\,\mathbb{P}(t_2,s/s'')\int\mathrm{d}\varphi\mathrm{d}\bar{t}\,\mathrm{d}K_X^2\,\frac{1}{k''^2-m_\pi^2}\mathcal{V}_2(Q^2,s',s'',K_X^2,\bar{t},t_2)\,, \tag{5.9}$$

where we have changed the phase-space integral $\mathrm{d}^3k'/2E_{k'}$ to an integral over $\mathrm{d}\bar{t}\mathrm{d}K_X^2\mathrm{d}\phi$, ϕ being the azimuthal angle of $\boldsymbol{p}'$ with respect to the plane defined by $\boldsymbol{k}$ and $\boldsymbol{k}'$.

In the c.m. frame $\boldsymbol{k}+\boldsymbol{k}'=0$, we can write

$$k'''^2 \underset{s'',s',Q^2\gg m_\pi^2}{\approx} \frac{(s'-s'')(s'-K_X^2)}{4s'}(1-\cos\Theta)\,,$$

where

$$\cos\Theta = \boldsymbol{p}\cdot\boldsymbol{k}'/|\boldsymbol{p}||\boldsymbol{k}|\,. \tag{5.10}$$

From (5.10) we see that the intermediate virtual pion is near its mass shell, when $s'\simeq s''$ or $s'\simeq K_X^2$. We now make the scale transformations $s''=\eta s'$ and $K_X^2=\eta_X s'$ and write (5.9) in the form

$$V'_{2\mathrm{abs}} = \frac{V_{\mathrm{pH}\pi}(t)\Delta_\pi(t)}{16(2\pi)^6\lambda^{1/2}(\omega'-1,1,0)}\int\frac{\mathrm{d}t_1\,\mathrm{d}t_2\theta(\lambda)}{\lambda^{1/2}(t,t_1,t_2)}N^{\pi\mathbb{P}}_{\mathrm{pH}}(t,t_1,t_2)G_{\pi\pi\mathbb{P}}$$

$$\times\Delta_\pi(t_1)\frac{1}{s'}\int\mathrm{d}\eta\,\frac{1}{\eta(1-\eta)}\left(\frac{s}{\eta s'}\right)^{\alpha' t_2}\int\mathrm{d}\varphi\mathrm{d}\bar{t}\mathrm{d}\eta_X\,\frac{4}{1-\eta_X}$$

$$\times\frac{1}{1-\cos\Theta(\bar{t},\varphi)}\,\mathcal{V}_2(Q^2,s',\eta',\eta_X s',\bar{t},t_2)\,. \tag{5.11}$$

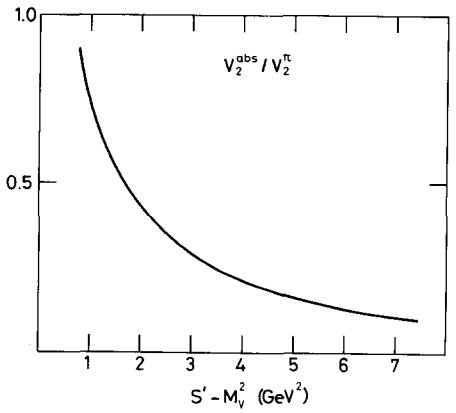

Fig. 15. Plot of ratio V_2^{abs}/V_2^{π} in the resonance region.

Comparing (5.11) with (5.6) we see that, for large s',

$$V'_{2abs} \lesssim \frac{1}{s'} V'_2 , \tag{5.12}$$

where in the deep inelastic region $s' = M_X^2 = (\omega' - 1)Q^2$. The initial-state absorption correction in fig. 12b can be treated in much the same way; however, it involves a completely different input, namely the six-point function shown in fig. 13b. Assuming this has similar scaling properties as $W^{\mu\nu}_{(3)}$, then, as far as the $s'^{-1} = 1/(\omega' - 1)Q^2$ behaviour is concerned, the same argument as above goes through. On the other hand, should this not scale, but rather grow like some power $(Q^2)^{\alpha}$ relative to the scaling behaviour, this would cause a serious violation of scaling in the total inclusive distribution ep → e + X in the large-ω region through the contributions from diagrams like that shown in fig. 14.

There are two extreme regions, where one might expect a different behaviour from that discussed above or at least where one has to argue differently, namely

(i) the resonance region $M_X^2 \lesssim 4$ GeV^2, and

(ii) the large ω' region, where one might try to describe the deep inelastic state itself by Regge exchanges.

We begin by considering the resonance region, since here the absorption corrections are most likely to be important. In order to make a quantitative estimate of the corrections in this region, one needs a more detailed knowledge of the inclusive structure functions $\mathcal{V}_2^{\pi}$ defined in (5.3). We shall make the following narrow resonance ansatz, which we suppose to be valid for large $q^2 = -Q^2$ and $s', s'' \ll Q^2$, namely

$$\mathcal{V}_2^{\pi} = \sum_v A(s', q^2, M_v^2) A^*(s'', q^2, M_v^2) \delta(K_X^2 - M_v^2) , \tag{5.13}$$

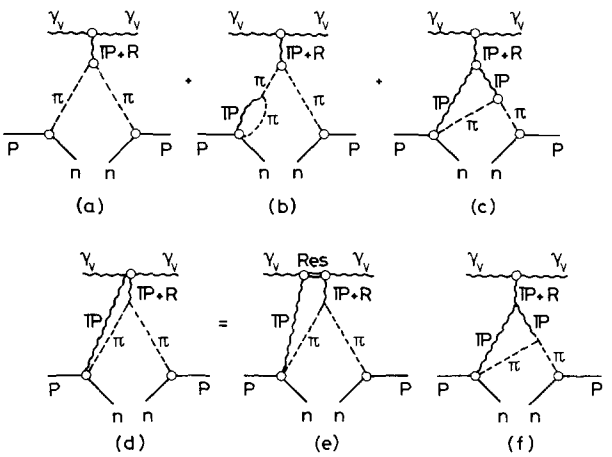

Fig. 16. (a)–(f) Show the OPE plus possible Regge-cut corrections, when the deep inelastic state is described by Regge exchange.

where $A(s', q^2, M_V^2)$ and $A^*(s'', q^2, M_V^2)$ are the residue functions at the pole at $K_X^2 = M_V^2$. In this region we have assumed the t-dependence drops out, which follows from, for example, the dual light cone model [24] ($Q^2 \gg s', M_X^2$). The absence of this t-dependence in (5.13) considerably simplifies eq. (5.11). In performing the $ds''(d\eta)$ integration, we note it is dominated by the region $s'' \approx s'$ and make a mean value approximation, in which we replace $A^*(s'', q^2, M_V^2)$ by $A^*(s', q^2, M_V^2)$. Finally, performing the two-dimensional integral over $dt_1 dt_2$, we obtain the following rough estimate of V_2^{abs} for a given resonance V:

$$\left|\frac{V_{2\text{abs}}}{V_2^{\eta}}\right| \approx \frac{c}{m_\pi^2 \Delta_\pi(t)} \frac{1}{64\pi} G_{\pi\pi\mathbb{P}} G_{\text{HH}\mathbb{P}} \frac{1}{\alpha'_\pi(s' - M_V^2)} \quad , \tag{5.14}$$

where we have assumed that the reggeon-particle amplitude $A_{\text{pH}}^{\pi\text{P}}$ (see eq. (5.1)) is dominated by the intermediate state H. If we allow a factor of 1.5 for the contributions of other intermediate states in $A_{\text{pH}}^{\pi\text{P}}$, then a crude upper estimate of the numerical constant c is $c \simeq 0.2$. In fig. 15 we have plotted the ratio $V_{2\text{abs}}/V_2^{\eta}$ for $t = 2m_\pi^2$, as given by (5.14), taking $\alpha'_{\text{P}} = 0.25$ GeV^2 and assuming the πH total cross section is about 20 mb. We see, in fact, that the absorption corrections can become important in the neighbourhood of the resonance. One should therefore make experimental checks for the level of the absorption corrections in the resonance region, following the suggestions of sect. 4.

Finally, we briefly consider the situation where we describe the deep inelastic state itself by Regge exchanges, which might be the appropriate description of the large-ω' region. The pure OPE corresponds to the triple-reggeon diagram shown in fig. 16a and one can envisage Regge-cut corrections of the form shown in fig. 16b

and c. The latter can be computed in a naive way using Gribov's reggeon calculus [37] and it is simple to see that in the region $s/Q^2 = 20-100$, $t \simeq t_{\min} < 5m_\pi^2$, only the diagrams which contain the pion pole are significant. The former simply correspond to vertex corrections associated with reggeized OPE and should be included in the proper parametrization of OPE. We have neglected diagrams of the form shown in fig. 16d, which decompose into two pieces shown in fig. 16e and f, because apart from the resonance piece (fig. 16e), they are already included in fig. 16c. The resonance part is neglected because of the assumed form factor behaviour for the photon-pomeron resonance vertex. We shall mention the consequences of relaxing the latter assumption in our concluding remarks, where we suggest how it might be experimentally tested.

6. Concluding remarks

Given reasonable statistics, we have discussed how the pion structure functions can be extracted from the inclusive distributions

$$\mu p \to \mu + n + \text{anything}\,, \tag{6.1}$$

$$\mu p \to \mu + \Delta^{++} + \text{anything}\,, \quad \Delta^{++} \hookrightarrow p^+\pi^+ \tag{6.2}$$

in the small-t region ($|t| < 0.1$ GeV^2). The data for $|t| > 0.1$ GeV^2 can be used to extract information on the deep inelastic structure of an unspecified virtual mesonic system. Here one might look for a universal behaviour by comparing the resulting structure functions (assuming factorization) for different detected hadrons and with the pion structure functions obtained from the small-t data.

The pomeron structure functions can be extracted from the inclusive distribution

$$\mu p \to \mu + p + \text{anything}\,, \tag{6.3}$$

where both the pomeron and pion exchange compete. We have based our analysis of the absorption corrections of the OPE contribution to (6.1) and (6.2) on the assumption that the photon-pomeron diffractive resonance transition vertex has a form factor $F_{\gamma_V \mathrm{PR}}(q^2)$. If the Drell-Yan relations hold for the pomeron structure functions, then we would expect the following threshold behaviour

$$F_2^{\pi}(\omega') \underset{\omega' \to 1}{\simeq} (\omega' - 1)^{2n-1}\,, \tag{6.4}$$

where n is defined by

$$F_{\gamma_V \pi \mathrm{R}}(q^2) \underset{|q^2| \to \infty}{\simeq} |q^2|^{-n}\,. \tag{6.5}$$

This means that in the small-ω' region the inclusive distribution (6.3) behaves like

$$\frac{d^2\sigma}{d\omega' dt} = p^2_{pp\pi}(t)\,\frac{1}{s}\left(\frac{s}{Q^2}\right)^{2\alpha_\pi(t)} c(\omega' - 1)^{2n-1} . \tag{6.6}$$

If $n = 0$, we see that this distribution will be singular as $\omega' \to 1$. Hence looking at the threshold behaviour of (6.3) as $\omega' \to 1$, suffices to check our basic assumptions, namely $n > 0$. From the latter it follows that the absorption corrections to the OPE mechanism in (6.1) and (6.3) are negligible in the deep inelastic region, except perhaps in the resonance region $\omega' \sim 1$ (see sect. 5).

We wish to thank U. Amaldi, F. Brasse, E. Gabathuler, G. Kramer, J.C. Polkinghorne, G. Preparata, H. Scott, F. Wagner, and particularly R. Worden, for informative discussions. We are also grateful to G. Preparata for reading the manuscript.

Note added: An attempt to extract the pion function from the existing ep data has been made by M. Chaichian and H.R. Rubinstein (private communication).

Appendix

We discuss here the interference between π and A_2 exchanges in $\gamma_v p \to \Delta^{++}(p^+\pi^+) + X$. For the $pA_2\Delta$ vertex we assume the same helicity structure as the $p\rho\Delta$ vertex corresponding to ρ-A_2 exchange degeneracy. The $p\rho\Delta$ vertex is assumed to correspond to a pure M_{1+} transition (cf. $p\gamma\Delta$), leading to the Stodolsky-Sakurai Δ-decay distribution for ρ-exchange, which also works well for A_2 exchange (see ref. [30]). In this case it is simple to show that the density matrices defined in (4.18) for the π-A_2 interference term are given in the Gottfried-Jackson system, by

$$\rho_{1-1} = \tfrac{1}{2} , \qquad \rho_{33} = \rho_{11} = \rho_{3-1} = \rho_{3-3} = 0 . \tag{A.1}$$

The angular distribution for the unpolarized cross section is given by (cf. eqs. (4.20)–(4.22)):

$$W^{\pi A_2}(\theta,\varphi) = \mathrm{Tr}\ \rho A(\theta,\varphi) = -i\,\mathrm{Im}\ D^{3/2}_{1/2\,1/2}(\theta,\varphi) D^{3/2}_{-1/2\,1/2}(\theta,\varphi) + D^{3/2}_{1/2\,-1/2}(\theta,\varphi) D^{3/2}_{-1/2\,-1/2}(\theta,\varphi) = 0 . \tag{A.2}$$

Hence there is no interference term between π and A_2 exchanges in the unpolarized inclusive cross section.

References

[1] J.D. Sullivan, Phys. Rev. D5 (1972) 1732.
[2] S.D. Drell and T.-M. Yan, Phys. Rev. Letters 24 (1970) 181.
[3] B. Richter, Proc. 17th Int. Conf. on high-energy physics, London, 1974, ed. J.R. Smith (Science Research Council, Didcot, 1974), p. IV-37.

[4] R.P. Feynman, Phys. Rev. Letters 23 (1969) 1415;
J.D. Bjorken and E.A. Paschos, Phys. Rev. 185 (1969) 1975;
P.V. Landshoff, J.C. Polkinghorne and R.D. Short, Nucl. Phys. B28 (1971) 225.
[5] For example, $pp \to \mu^+\mu^- + X$:
S.D. Drell and T.-M. Yan, Phys. Rev. Letters 25 (1970) 316;
M.B. Einhorn and R. Savit, NAL reports NAL-Pub-74/35-THY, NAL-Pub-74/41-THY (1974);
H. Paar and M. Paschos, NAL report NAL-Pub-74/29-THY (1974);
J.H. Christenson et al., Phys. Rev. D8 (1973) 2016.
$\gamma p \to \gamma + X$:
J.D. Bjorken and E.A. Paschos, ref. [4];
D.O. Caldwell et al., paper submitted to the 17th Int. Conf. on high-energy physics, London, 1974.
[6] S.J. Brodsky and G.R. Farrar, Phys. Rev. Letters 31 (1973) 1153.
[7] G. Preparata, A possible way to look at hadrons: the massive quark model, Lectures given at the "Ettore Majorana" School of Physics, Erice, 1974, to be published.
[8] A. Suri, Phys. Rev. D4 (1971) 510;
R. Gatto, P. Menotti and I. Vendranini, Nuovo Cimento Letters 4 (1974);79;Ann. of Phys. 79 (1973) 1;
R. Gatto and G. Preparata, Nucl. Phys. B47 (1972) 313; (Erratum B73 (1974) 54);
P.V. Landshoff and J.C. Polkinghorne, Phys. Rev. D6 (1972) 3708;
H.D. Dahmen and F. Steiner, Phys. Letters 43B (1973) 21.
[9] V.N. Gribov and L.N. Lipatov, Phys. Letters 37B (1971) 78; Yad. Fiz. 15 (1972) 781; Sov. J. Nucl. Phys. 15 (1972) 438;
G. Schierholz, Phys. Letters 47B (1973) 374.
[10] S.M. Berman, Phys. Rev. 135 (1964) 1249.
[11] A.H. Mueller, Phys. Rev. D2 (1970) 2963.
[12] P. Goddard and A.R. White, Nuovo Cimento 1A (1971) 645;
C.E. Jones, F.E. Low and J.L. Young, Phys. Rev. D4 (1971) 2358;
C.E. DeTar and J.H. Weis, Phys. Rev. D4 (1971) 3141;
H.D.I. Abarbanel and A. Schwimmer, Phys. Rev. D6 (1972) 3018.
[13] N.S. Craigie and G. Kramer, Nucl. Phys. B82 (1974) 69.
[14] P. Hoyer, Proc. 17th Int. Conf. on high-energy physics, London, 1974, ed. J.R. Smith (Science Research Council, Didcot, 1974), p. I-158.
[15] K.C. Moffeit et al., Phys. Rev. D5 (1972) 1603;
H. Burfeindt et al., Phys. Letters 43B (1973) 345;
C. Berger et al., Phys. Letters 47B (1973) 377;
[16] F.T. Dao et al., Phys. Rev. Letters 30 (1973) 34.
[17] N.S. Craigie, J. Körner and G. Kramer, Nucl. Phys. B68 (1974) 509.
[18] E. Gotsman and U. Maor, Nucl. Phys. B57 (1973) 574.
[19] R.J.N. Phillips, Proc. Amsterdam Int. Conf. on elementary particles, eds. A.G. Tenner and M.J.G. Veltman (North-Holland, Amsterdam, 1972) p. 110.
[20] Y. Frishman, Proc. 16th Int. Conf. on high-energy physics, Chicago-Batavia, 1973, eds. J.D. Jackson and A. Roberts (NAL, Batavia, Ill., 1973) vol. 4, p. 119.
[21] C.G. Callan and D.J. Gross, Phys. Rev. Letters 22 (1969) 156.
[22] G. Schierholz and M.G. Schmidt, Phys. Letters 52B (1974) 467.
[23] E.D. Bloom, Proc. 6th Int. Symp. on electron and photon interactions, Bonn, 1973, eds. W. Pfeil and H. Rollnik (North-Holland, Amsterdam, 1974) p. 227.
[24] G. Schierholz and M.G. Schmidt, Phys. Rev. D10 (1974) 175.
[25] D. Chew, M. Tabak and F. Wagner, Lawrence Berkeley Laboratory report No. LBL-3396 (1974).

[26] V. Barger, Proc. 17th Int. Conf. on high-energy physics, London, 1974, ed. J.R. Smith (Science Research Council, Didcot, 1974) p. I-193.
[27] K. Gottfried and J.D. Jackson, Nuovo Cimento 33 (1964) 309.
[28] J.J. Sakurai and L. Stodolsky, Phys. Rev. Letters 11 (1963) 90.
[29] Y. Hara, Phys. Rev. 140 (1965) B178.
[30] G.F. Fox and C. Quigg, Stony Brook report No. ITP-SB-73-22 (1973).
[31] D.F. Grether and G. Gidal, Phys. Rev. Letters 26 (1971) 792.
[32] F. Wagner, private communication.
[33] N.S. Craigie and G. Kramer, Nucl. Phys. B75 (1974) 509.
[34] S. Treiman and C.N. Yang, Phys. Rev. Letters 8 (1962) 140.
[35] H.H. Bingham, in Proc. 11th Cracow School of Theoretical Physics (Cracow, 1971) vol. 1, p. 50.
[36] For example, Chan Hong-Mo, H.I. Miettinen and R.G. Roberts, Nucl. Phys, B54 (1971) 411.
[37] V.N. Gribov, JETP (Sov. Phys.) 26 (1968) 414..